J. Eng. Technol. Sci., Vol. 54, No. 3, 2022, 220308

Experimental and Theoretical Analysis of Throughput of MIMO PLC Network

Abdelmounim Hmamou[1], Mohammed El Ghzaoui[2], Jaouad Foshi[1] & Jamal Mestoui[2]

[1]ERTTI Laboratory, Moulay Ismail University, BP 509 Boutalamine, Errachidia, Morocco
[2]Faculty of Sciences Dhar El Mahraz-Fes, Sidi Mohamed Ben Abdellah University, Fes, B.P. 1796 Fès-Atlas, Morocco
*E-mail: hmamou0512@gmail.com

Highlights:

- The use of the MTL theory to obtain a new method of calculating the MIMO CTF.
- The impact of load household appliances connected to sockets in a MIMO PLC network on throughput (MIMO PLC channel capacity) and communication reliability.
- The type of socket has a significant impact on the performance of the MIMO PLC system.

Abstract. In this study, we mainly focused on a theoretical analysis of HomePlug 1.0 and an experimental analysis of modem data rates through a section of a PLC network with several configurations. We introduce the utilization of the MIMO technique to increase the throughput over a PLC channel. Besides, we propose a MIMO PLC channel model to evaluate the channel transfer function of MIMO PLC. We used an equivalent per-unit-length model of the indoor power line network to characterize the three-conductor cable. Based on this mathematical model, we analyzed the throughput of the PLC network with different household appliances. The equivalent circuit of each appliance is also given. The simulation results showed that the throughput is influenced by household appliances connected to the sockets of a MIMO PLC network. Moreover, we also compared the throughput between single and multi-antenna systems. Based on the simulation results, we found that the data rate increased with frequency. In addition, the performance of the MIMO PLC system was almost 90% higher than that of a SISO PLC system in terms of channel capacity.

Keywords: *data rate; HomePlug 1.0; MIMO PLC network; PLC network; throughput.*

1 Introduction

The electrical grid is increasingly becoming a smart grid tank to single and multiple power line communication (PLC) modems. It is now possible to share Internet access at high data rates with various devices connected to the power grid. Recently, the HD-PLC Alliance of Fukuoka, Japan has launched the Global

Received June 20th, 2021, 1st Revision August 30th, 2021, 2nd Revision September 17th, 2021, Accepted for publication November 10th, 2021.
 ISSN: 2337-5779, DOI: 10.5614/j.eng.technol.sci.2022.54.3.8

Strategy Preparatory Office. This group aims to support the acceleration of the transition to IoT. This will lead to a considerable increase in the need for high-speed PLC in various systems, such as building automation systems, smart meter systems, factory automation systems, smart street lighting systems, smart city systems, smart home systems, solar power generation systems, etc.

In contrast, PLC channels introduce strong signal attenuation, as well as a large sources of noise, which degrade the performance of PLC modems [1]. For example, HomePlug Turbo and AV provide a theoretical data rate of 5 to 85 Mbit/s and 10 to 200Mbit/s, respectively, for a useful throughput of 1 to 20 Mbit/s and 5 to 60 Mbit/s, respectively. This decrease in data rate can be explained by two causes. Firstly, the PLC channel is a harsh environment for signal transmission. Secondly, the size of the frame headers used in HomePlug and the use of a number of mechanisms to enable a reliable transmission in an electrical environment contribute to this, because part of the transmitted data is used for the control and management of the transmission. Adhering to a set of recommendations and specifications (as part of ITU-T G.hn and HomePlug AV2), and using eigenbeamforming (EBF), it is possible to double the throughput when moving from a SISO PLC configuration to a MIMO PLC configuration [2]. A MIMO configuration is theoretically able to increase the capacity of wireless communication links as compared to a SISO configuration [3]. Existing indoor PLC systems (such as SISO) use only two wires (phase and neutral) of the mains network, while MIMO additionally utilizes the protective earth wire in order to achieve maximum throughput. However, major issues still exist in PLC networks due to signal transmission-reflection, different network cables, complex topologies, and the variety of loads connected across the sockets [4].

Several studies have been carried out on PLC networks in order to enhance the performance of this technology. In Ref. [5], the capacity of the MIMO PLC channels was analyzed in a topology where the neutral and the protective earth wires were short-circuited in the main network. Corchado, *et al.* in [6] studied the influence of several elements, such as the impedance of the devices connected to the sockets of the power grid and various distances between the conductors and light switches on the performance of a MIMO PLC network. In [7], the MIMO PLC channel capacity is broadly analyzed and a comparison between SISO and MIMO channel capacity is proposed. The throughput in a section of a PLC network is analyzed in [8]. Duan, *et al.* [9] concluded that the influence of differential mode radiation can be ignored, whereas common mode radiation must be considered as the main factor affecting the transmission characteristics of MIMO PLC channels in the 1-100MHz frequency band [3-5]. Ref. [10] proposes an algorithm to improve the performance of the MIMO PLC channels based on a partial transmission sequence (PTS). This algorithm makes it possible to attenuate the noise in these types of channels. Ref. [11] compares the capacity

of PLC channels with the frequency response for different modeling techniques. Another technique for the same purpose is proposed in Ref. [12], called Hybrid Coding-Multiple Input Multiple Output-Orthogonal Frequency Division Multiplexing (HC-MIMO-OFDM), which also efficiently increases the transmission bit rate and reduces the effect of impulsive noise. Ref. [13] studied the effects of the correlation between different paths in MIMO PLC on the channel capacity in a PLC system utilizing Space-Time Output-Orthogonal Frequency Division (ST-OFDM) and Space-Time Parallel Cancellation Output-Orthogonal Frequency Division Multiplexing (STPC-OFDM) channel models. The achievable data rates were calculated and systematically analyzed under the effects of the distribution lines, connected loads, noise models, etc. It was demonstrated that MIMO systems outperform SISO systems. The authors of [14] investigated the feasibility of a smart metering system based on narrowband power line communications. The obtained results were measured to validate the efficiency of the proposed methods. In [15,16], the authors present a useful mathematical formulation for the input-output relation by means of matrices of a transmitter and receiver system based on windowed OFDM. The windowed OFDM was analyzed in terms of bit error rate (BER) and throughput. The effect of household appliances connected over a PLC-MIMO grid considering noise was classified in five classes in [17]. Within this classification, while also taking into account the protective earth wire, household appliances can be subdivided into two types, especially when using MIMO PLC technology, i.e., those connected by a three-pin plug (for phase and neutral plus earth) and those connected by a two-pin plug to sockets without earth.

In this paper, we will show the main effects of the utilization of the protective earth connection in a MIMO PLC system on the throughput of a MIMO PLC channel. Based on the above analysis, the PLC network is a fairly new approach that is still maturing, making it a promising technique for near-future applications. We propose a channel model for the MIMO PLC system. Based on this model, we analyzed the performance of the proposed MIMO PLC network in terms of throughput. We also provide an equivalent circuit for each electric appliance to see its impact on the attenuation of the transfer function as well as on the data rate of the proposed configuration. A performance comparison between SISO PLC and MIMO PLC is also given. This comparison revealed the superiority of MIMO PLC systems against conventional SISO PLC systems.

This article is organized as follows. In Section 2, we present a theoretical study of the throughput data rate in the HomePlug 1.0 standard. In Section 3, the useful throughput measurement of a SISO PLC network in the presence of different types of household appliance impedances is analyzed. In Section 4, we use the multi-conductor transmission line (MTL) theory to calculate the transfer function

of our structure and to determine the expression of MIMO PLC channel capacity. In Section 5, we present and discuss the results of our simulation.

2 Theoretical Data Rate of Homeplug1.0

If we look at the complete structure of the physical layer frame in HomePlug 1.0 that is permanently exchanged between the PLC devices (Figure 1), we notice that it consists of a number of elements surrounding the long data frame, including the data from the higher-level protocol layers forming the Open Systems Interconnection (OSI) model. In terms of time length, the HomePlug1.0 frame can be quantified by minimum and maximum values, with a fixed part (header), a variable data part, and a part used for contention periods with regard to the Carrier Sense Multiple Access/Collision Avoidance (CSMA/CA) process, as shown in Table 1. Therefore, the HomePlug1.0 frame consists of long data frames (which comprise the data of the MAC frames) and short data frames (which comprise the response information from other PLC devices). Keep in mind that the average time of a HomePlug1.0 frame is 1.600 µs. From the point of view of physical layer modulation techniques, the HomePlug1.0 data frame consists of OFDM symbols. These symbols form blocks that, in turn, constitute the complete framework.

Figure 1 illustrates the respective times of these various OFDM blocks. The complete frame time is defined by adding the various OFDM symbol block times. This makes it possible to calculate the maximum possible transmission speed and the bit rate of the data link layer. The time of the frame is: $T_{Frame} = (3 \times 35.84 + 3.5 \times 35.84 + 1153.5 + 26 + 72)\,\mu s = 1534.86\,\mu s$. With a 2705 bytes frame, the maximum transmission speed is obtained in the following way: $\mathrm{D_{theoretical}} = 2705\left(\frac{8\mathrm{bits}}{1534.86\mu\mathrm{s}}\right) = 14.1\mathrm{Mbit/s}$ With an Ethernet data frame with a maximum length of 1500 bytes, the maximum data rate is the following: $\mathrm{D_{theoretical}} = 1500\left(\frac{8\mathrm{bits}}{1534.86\mu\mathrm{s}}\right) = 7.81\mathrm{Mbit/s}$ However, this flow does not correspond to reality.

In PLC, data sending must comply with certain rules related to the CSMA/CA access method, which is based on a number of mechanisms that generate a large overhead. It can be said that a PLC network never reaches the capacity mentioned in the specifications. If the information is transmitted at a speed of 14 Mbit/s, the number of bits useful to the user is only approximately half of the gross capacity of the electrical interface. To confirm these results, the next paragraph will focus on flow measurement on a PLC network using an 85-Mbps and a 200-Mbps PLC adapter.

Table 1 HomePlug 1.0 frame time length.

	Fixed (header)		Variable (data)		Contention (CSMA/CA)	Time length
Min	205.52 µs µs	+	313.5µs	+	N*35.84 µs	=519.02 µs + N*35.84
Max	205.52 µs µs	+	1489.5µs	+	N*35.84 µs	=1692.02+ N*35.84

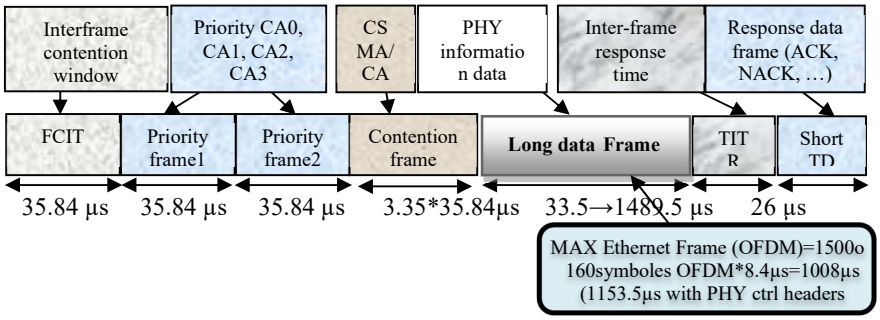

Figure 1 Complete HomePlug 1.0 frame.

2.1 Experimental Analysis of Modem Data Rate Through a Section of a PLC Network

In this section, we focus on the performance of an 85-Mbps and a 200-Mbps PLC modems in terms of throughput and robustness against disturbances generated directly and indirectly on a PLC network section without the presence of an extension and without branch, and also in the presence of an extension and without branch. The test circuit, represented in Figure 2 below, consisted of two PLC modems connected to two computers for data transfer via the section, according to the following configuration: T (transmitter) and R (receiver) sockets.

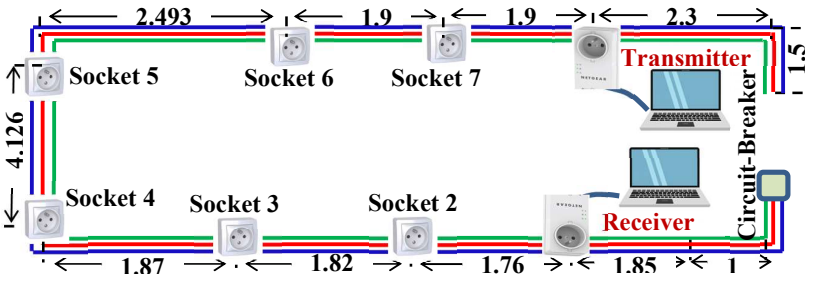

Figure 2 Experimental PLC network.

2.2 Throughput Measurement in a Section of a PLC Network With and Without Extension under Different Types of Loads

In Figure 3, we show the data rates measured in a section of a PLC network with length LC = 5.5 m, with and without extension branch (length Lex = 2.5 m) for different types of loads.

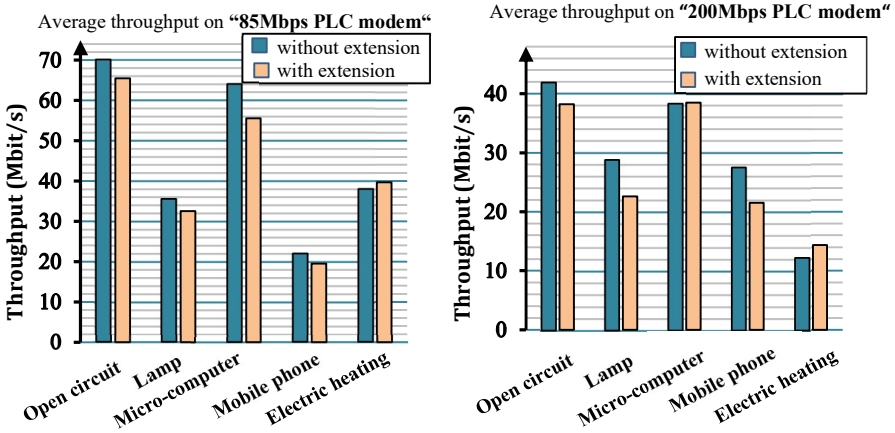

Figure 3 Variation of a channel throughput with and without extension branch according to different types of loads for an 85-Mbps PLC modem and a 200-Mbps PLC modem.

The decrease of the channel's capacity was caused by increasing the length of the branch (an extension cable), by the nature of the load connected to the branch, and also by the distance between the transmitter and the receiver. As demonstrated in this paper, the load has an important effect on the throughput. Furthermore, the impact of the extension cable length on the throughput has been already discussed in [8]. Table 2 shows the impact of the length of the extension cable on the throughput, as demonstrated in [8]. From this table, a slight decrease in throughput can be seen when the length of the branch increases from 15 to 45 meters. Therefore, the length of the extension cable did not have a significant effect on the throughput.

Table 2 Influence of extension cable length on throughput.

Length of extension (m)	15	25	35	45
Throughput (Mbps)	3.12	3.03	2.96	2.93

In the presence of a microcomputer or an open circuit, the throughput level does not change very much. The nature of the load is the most important factor. Indeed,

in the presence of load type, there is a significant drop, which can reach 17 Mbps (85-Mbs PLC modem) and 20 Mps (200-Mbs PLC modem), which corresponds to a loss of 79% and 90%, respectively. Figure 3 reveals that the throughput level obtained was better with the 85-Mbs modem than with the 200-Mbs modem. This could be mainly due to modem technology, since the measurements were carried out under the same conditions.

3 MIMO PLC System

MIMO communication is an established technique in radio transmission systems and is equally applicable to PLC by replacing the transmit and receive antennas with signal feed and receive ports, and a radio channel with electrical wiring. It is quite common across the world to use a three-wire electrical system, i.e. P, N, and PE, for indoor PLC networks. As a result, there are three different feeding possibilities, i.e., N to P, N to PE, and P to PE, as shown in Figure 4.

Figure 4 Indoor MIMO PLC channel.

Conventional SISO PLC networks use only the P-N port for the transmission and reception of data. Therefore, in the case of MIMO PLC, the PE wire is also used in addition to the P and N wires to transmit and receive data. Nevertheless, due to Kirchhoff's law, only two ports can be used simultaneously to transmit data. At the receiver, all three different receiving ports can be used. In addition, the common mode (CM) path can also be employed as a fourth receiving port.

3.1 Transfer Function of MIMO PLC Channel

The data through the power line can be transmitted through a differential signal between P-N or P-E or N-E. For SISO communication, the signal is fed through any one the ports. For MIMO communication, the signal is fed through multiple ports simultaneously. We can use the equivalent per-unit-length model of an indoor power line network, as shown in Figure 5, to characterize the three-conductor cable.

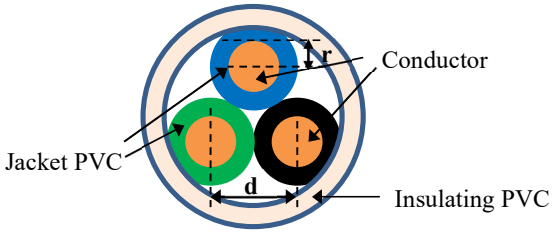

Figure 5 Symmetric cable cross-section (left) and per-unit length equivalent (right) of a three-wire indoor power line.

Kirchhoff's laws are used to derive the formulas expressing the voltage and current in phasor form for the elementary section of the line, which is shown in Figure 6. More detailed information on the general solution of the differential equations for such lines can be found in [18-20].

$$\frac{\partial V(x)}{\partial x} = -(R_{MIMO} + j2\pi f L_{MIMO})I(x) \quad (1)$$

$$\frac{\partial I(x)}{\partial x} = -(G_{MIMO} + j2\pi f C_{MIMO})V(x) \quad (2)$$

where x denotes the position at the conductor. One of the conductors is identified as the reference conductor. The matrices $\boldsymbol{R_{MIMO}}$, $\boldsymbol{L_{MIMO}}$, $\boldsymbol{G_{MIMO}}$ and $\boldsymbol{C_{MIMO}}$ have dimension (2,2), where 2 is the number of conductors without the reference conductor, and they are symmetrical with respect to the diagonal. The resistance, inductance, conductance, and capacitance in terms of Ω/m, H/m, F/m and S/m respectively are specified as per-unit-length parameters. These are obtained from the transmission line theory.

$$R_{MIMO} = \begin{bmatrix} R_P + R_E & R_E \\ R_E & R_N + R_E \end{bmatrix} \quad ; \quad L_{MIMO} = \begin{bmatrix} L_P & L_M \\ L_M & L_N \end{bmatrix} ;$$

$$C_{MIMO} = \begin{bmatrix} C_{PE} + C_{PN} & -C_{PN} \\ -C_{PN} & C_{NE} + C_{PN} \end{bmatrix} ; \quad G_{MIMO} = \begin{bmatrix} G_{PE} + G_{PN} & -G_{PN} \\ -G_{PN} & G_{NE} + G_{PN} \end{bmatrix}$$

The computation of the per-unit-length parameter matrices and can be done in an analytical way for the symmetric cable geometry shown in Fig 5. Assuming that the phase, neutral and ground wires have the same geometrical and electrical properties, we have that: $R = R_P = R_N = R_E$; $L = L_P = L_N = 2L_M$; $C = C_{PE} = C_{NE} = C_{PN}$ and $G = G_{PE} = G_{NE} = G_{PN}$

where the resistance R, inductance L, capacitance C and conductance G can be obtained from the following relationships:

$$R = \begin{cases} \frac{1}{\pi\sigma r^2} & r \le 2\delta \\ \frac{1}{2r}\sqrt{\frac{\mu_0 f}{\pi\sigma}} & r > 2\delta \end{cases} \quad ; \quad L = \frac{\mu_0\mu_r}{\pi} acosh\left(\frac{d}{2r}\right) + \frac{R}{2\pi f};\ (\mathrm{H}/m)$$

$$C = \frac{\pi\varepsilon_0\varepsilon_r}{acosh\left(\frac{d}{2r}\right)}\ (\mathrm{F}/m) \quad ; \quad G = 2\pi f C\ tan(\delta)\ \ (\mathrm{S}/m),$$

where **r** is the radius of the conductors, d is the distance between the conductors, σ is the electric conductivity of the conductors, μ is the magnetic permeability ($\mu = \mu_0\mu_r$), **ε** is the dielectric constant ($\varepsilon = \varepsilon_0\varepsilon_r$), and $\delta = \frac{\mathbf{1}}{\sqrt{\pi f \mu_0 \mu_r \sigma)}}$ is the skin depth.

To simplify the notation, the impedance and admittance matrices of the transmission lines are defined as follows:

$$Z = R_{MIMO} + j2\pi f L_{MIMO} \quad \text{and} \quad Y = G_{MIMO} + j2\pi f C_{MIMO}$$

By means of a first derivative and a substitution, we obtain the multi-conductor transmission-line (MTL) equations in Eqs. (3) and (4):

$$\frac{\partial^2 V(x)}{\partial x^2} = ZYV(x) \tag{3}$$

$$\frac{\partial^2 I(x)}{\partial x^2} = YZI(x) \tag{4}$$

Introducing the substitutions $Vm = T^{-1}V$ and $ZY = T\Lambda T^{-1}$ it is possible to define Eq. (3) as in Eq. (5):

$$\frac{\partial^2 V_m(x)}{\partial x^2} = \Lambda T^{-1}V(x) = \Lambda V_m(x) \tag{5}$$

where T is the eigenvector of matrix ZY, and Λ is matrix, which has the eigenvalues of matrix ZY on the diagonal.

By introducing the matrix $\Gamma = \sqrt{\Lambda}$ we can find the general solution to these equations in Eq. (6):

$$Vm(x) = e^{-\Gamma x}\, V_m^+ \ + \ e^{\Gamma x}\ V_m^-, \tag{6}$$

where $\boldsymbol{V_m^+}$ and $\boldsymbol{V_m^-}$ are voltage vectors whose coefficients are determined from the boundary conditions. Finally, taking into account the above formulas, it is easy to obtain the expression for the current vector and the voltage vector:

$$V(x) = T(e^{-\Gamma x}\, V_m^+ \ + \ e^{\Gamma x}\ V_m^-)\ and\ (12) I(x) = Z_C^{-1} T(e^{-\Gamma x}\, V_m^+ - \ e^{\Gamma x}\ V_m^-)$$

where $Z_C = T\Gamma^{-1}T^{-1}Z$ is the characteristic impedance matrix.

At the input and output of transmission line of length L and after modifying, we can write:

$$\begin{pmatrix} V_{out} \\ I_{out} \end{pmatrix} = \underbrace{\begin{bmatrix} M_{11} & M_{12} \\ M_{21} & M_{22} \end{bmatrix}^{-1}}_{\mathrm{M(L)}} \begin{pmatrix} V_{in} \\ I_{in} \end{pmatrix} = \Phi \begin{pmatrix} V_{in} \\ I_{in} \end{pmatrix}, \quad (7)$$

where $\mathrm{M_{11}} = \frac{1}{2}\mathrm{T}(e^{\Gamma L} + e^{-\Gamma L})\mathrm{T}^{-1}$; $\mathrm{M_{12}} = \frac{1}{2}\mathrm{T}(e^{\Gamma L} - e^{-\Gamma L})\mathrm{T}^{-1}\mathrm{Z_C^{-1}}$;

$\mathrm{M_{21}} = \frac{1}{2}\mathrm{Z_C^{-1}T}(e^{\Gamma L} - e^{-\Gamma L})\mathrm{T}^{-1}$ and $\mathrm{M_{22}} = \frac{1}{2}\mathrm{Z^{-1}T}(e^{\Gamma L} + e^{-\Gamma L})\mathrm{T}^{-1}\mathrm{Z}$,

where M(L) denotes the chain-parameter matrix for a line segment of length L, and $\Phi = \begin{bmatrix} \Phi_{11} & \Phi_{12} \\ \Phi_{21} & \Phi_{22} \end{bmatrix}$ is the inverse matrix of matrix M. Using the MIMO PLC network shown in Figure 7, the $\boldsymbol{V_{in/out}} = \begin{pmatrix} \boldsymbol{V^1_{in/out}} \\ \boldsymbol{V^2_{in/out}} \end{pmatrix}$ are the transmitter/receiver voltages and $\boldsymbol{Z_{in/out}} = \begin{bmatrix} \boldsymbol{Z^{11}_{in/out} + Z^{12}_{in/out}} & \boldsymbol{-Z^{12}_{in/out}} \\ \boldsymbol{-Z^{12}_{in/out}} & \boldsymbol{Z^{22}_{in/out} + Z^{12}_{in/out}} \end{bmatrix}$ are the transmitter/receiver equivalent impedance matrices. $\mathbf{L_i}$ is the length of the wire from the source to a branch **i** or between two branches, $\mathbf{Lb_i}$ is the length of a branch **i**. $\boldsymbol{Z_{bi}} = \begin{bmatrix} \boldsymbol{Z^{11}_{bi} + Z^{12}_{bi}} & \boldsymbol{-Z^{12}_{bi}} \\ \boldsymbol{-Z^{12}_{bi}} & \boldsymbol{Z^{22}_{bi} + Z^{12}_{bi}} \end{bmatrix}$ is the load impedance matrix of a branch **i**.

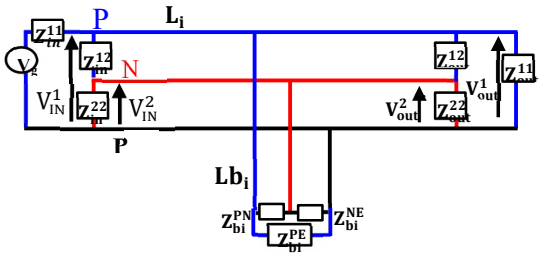

Figure 6 Transmission line model of our indoor circuit.

The branch cable terminated by the load impedance $\boldsymbol{Z_{bi}}$ can be considered to be an equivalent load impedance matrix $\boldsymbol{z_{bi}}$:

$$z_{bi} = (M_{11}Z_{bi} + M_{12})((M_{21}Z_{bi} + M_{22})^{-1}, \quad (8)$$

where M_{11}, M_{12}, M_{21}, and M_{22} are the transmission parameter matrices of a branch *i* can be computed with the following expressions:

$$M_{11} = M_{22} = \begin{bmatrix} 1 & 0 \\ 0 & 1 \end{bmatrix}; \quad M_{12} = \begin{bmatrix} 0 & 0 \\ 0 & 0 \end{bmatrix} \; and \; \; M_{21} = {z_{bi}}^{-1}$$

The source of the transmission line can be computed with the following expressions:

$$M_{11} = M_{22} = \begin{bmatrix} 1 & 0 \\ 0 & 1 \end{bmatrix}; \; M_{12} = z_{bi} \; and \; \; M_{21} = \begin{bmatrix} 0 & 0 \\ 0 & 0 \end{bmatrix}$$

From the matrices obtained for each part, the whole network is given by:

$$M_{Total} = \prod_{k=0}^{n} M_k = M_0 \times M_1 \times \dots M_{n-1} \times M_n, \tag{9}$$

where M_i is the transmission parameter matrix of segment **i** of length $\mathbf{l_i}$. Therefore, the 4×4 matrix M_{Total} can be defined as: $M_{Total}^{ij} = \begin{bmatrix} M_{11}^{ij} & M_{12}^{ij} \\ M_{21}^{ij} & M_{22}^{ij} \end{bmatrix}$

Combining with Eq. (7) and substituting for $Vout$ at the end of network we can write:

$$V_{out} = \Phi_{11} V_{in} + \Phi_{12} I_{in} \quad \text{and}$$

$$Z_{out} I_{out} = Z_{out} \Phi_{21} V_{in} + Z_{out} \Phi_{22} I_{in}$$

After modifying:

$$V_{out} = \Phi_{11} V_{in} + \Phi_{12} I_{in} \text{ and } (Z_{out} \Phi_{22})^{-1} (V_{out} - Z_{out} \Phi_{21} V_{in}) = I_{in}$$

After substituting $\boldsymbol{I_{in}}$ into the expression of $\boldsymbol{V_{out}}$ we get the following expression:

$$V_{out} = \Phi_{11} V_{in} + \Phi_{12} {\Phi_{22}}^{-1} {Z_{out}}^{-1} V_{out} - \Phi_{12} {\Phi_{22}}^{-1} \Phi_{21} V_{in}$$

After modifying we can write:

$$\left(I - \Phi_{12} {\Phi_{22}}^{-1} {Z_{out}}^{-1}\right) V_{out} = \left(\Phi_{11} - \Phi_{12} {\Phi_{22}}^{-1} \Phi_{21}\right) V_{in}$$

This expression can be simplified to:

$$V_{out} {V_{in}}^{-1} = \left(I - \Phi_{12} {\Phi_{22}}^{-1} {Z_{out}}^{-1}\right)^{-1} \left(\Phi_{11} - \Phi_{12} {\Phi_{22}}^{-1} \Phi_{21}\right)$$

Finally, the MIMO PLC channel transfer function of our power line network (with three wires) is given by:

$$H^{ij} = \left(I - \Phi_{12}^{ij}\left(\Phi_{22}^{ij}\right)^{-1}\left(Z_{out}^{ij}\right)^{-1}\right)^{-1}\left(\Phi_{11}^{ij} - \Phi_{12}^{ij}\left(\Phi_{22}^{ij}\right)^{-1}\Phi_{21}^{ij}\right) \quad (10)$$

where,

$$\Phi_{11}^{ij} = \left(M_{Total}^{ij}\right)^{-1}(1,1);\ \Phi_{12}^{ij} = \left(M_{Total}^{ij}\right)^{-1}(1,2);$$
$$\Phi_{21}^{ij} = \left(M_{Total}^{ij}\right)^{-1}(2,1)\quad ;\quad \Phi_{22}^{ij} = \left(M_{Total}^{ij}\right)^{-1}(2,2)$$

I is the 2×2 identity matrix, and $H^{ij} = \begin{bmatrix} h_{N\,PE-N\,PE} & h_{N\,PE-P\,PE} \\ h_{P\,PE-N\,PE} & h_{P\,PE-P\,PE} \end{bmatrix}$

3.2 Transfer Function and Throughput of MIMO PLC Channel

Studying the impact of the impedance of household electrical appliances on the throughput in the PLC network can be realized by calculating the channel capacity [21].

The SISO channel capacity is given by the following equation:

$$C_{SISO} = \Delta f \sum_{n=1}^{N} Log_2\left(1 + \frac{P_{Tx}(f_n).|h_{ii}(f_n)|^2}{N_{Rx}(f_n)}\right), \quad (11)$$

where $\boldsymbol{\Delta f}$ is the carrier frequency, N is the number of carrier frequencies, $\boldsymbol{h_{ii}(f_n)}$ is the co-channel transfer function, and $\boldsymbol{P_{Tx}}$ and $\boldsymbol{N_{Rx}}$ are the power spectral density (PSD) and the noise spectral density (NSD), respectively.

The 2×2 $MIMO$ channel capacity is given by the following equation:

$$C_{MIMO} = \Delta f \sum_{m=1}^{2}\sum_{n=1}^{N}\left[Log_2\left(1 + \frac{P_{Tx}(f_k).|\eta_m(f_k)|^2}{2\,.N_{Rx}(f_k)}\right)\right] \quad (12)$$

where **2** is the number of transmit ports, $\boldsymbol{\eta_m}$ are singular values (SVD) of H^{ij}. The SVD are obtained by $H^{ij} = U\Psi V$, where U and V are unitary matrices and $\Psi = \text{diag}(\boldsymbol{\eta_1(f_k)}, \boldsymbol{\eta_1(f_k)})$.

In a wireless context, as discussed in [22], the performance of a MIMO system is better than that of a SISO system in terms of throughput.

4 Results and Discussion

The real PLC channel considered in this work is represented in Figure 7. The cable used in the power line network has a cross-sectional area of 2.5 mm^2 and consists of multiple branches distributed across the line length, which are connected with various domestic appliances. These appliances are a lamp, a micro-computer charger, a mobile phone charger, and an electric heater. Based

on the load connected or the ampere rating of the plug socket, the cross-section of the wiring also differs.

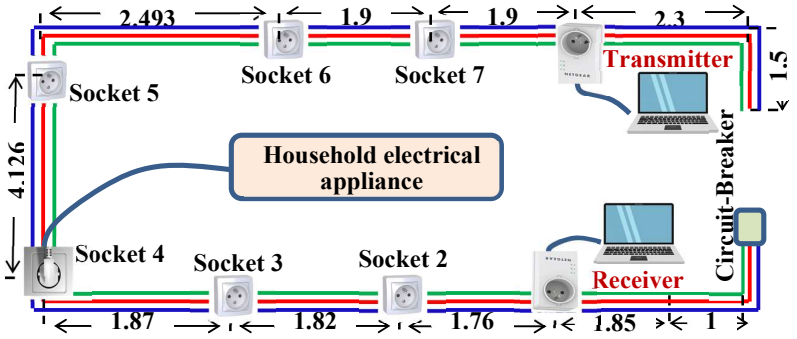

Figure 7 Experimental in-home PLC network.

The household electric appliances were classified into five classes according to their input impedances. These impedances were modeled as a series connection of parallel RLC circuits, because most of the input impedances in operating state and non-operating state do not change. Thus, to model the input impedances of the household electric appliances we have to consider the approach that was adopted in [17,23]. Figures 8(a) and 8(b) show the equivalent circuits for the electric heater and the micro-computer, respectively. These two appliances have a protective earth (PE) connection. Figures 8(c) and 9 show the equivalent circuits for the lamp and the mobile phone charger, respectively. The latter two appliances did not have a PE connection. All four impedances were chosen to see their impacts on the channel transfer function and then to analyze their influences on the throughput data rate of the MIMO PLC network.

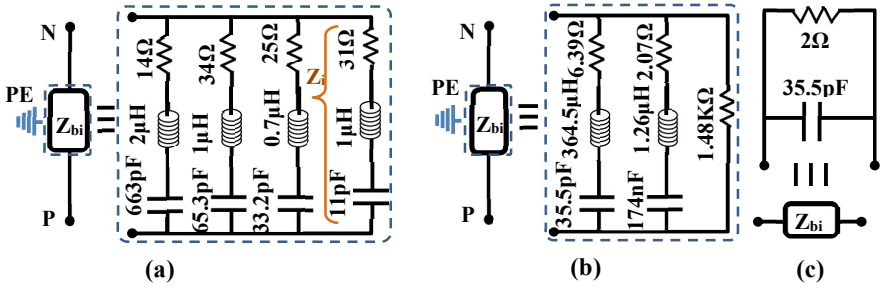

Figure 8 Equivalent impedance of (a) electric heater, (b) micro-computer, and (c) lamp.

The impedance of the equivalent circuit for the electric heater was modeled by the circuit shown in Figures 8 and 9. Its input impedance is given by:

$$Z_{bi} = 1/\left(\frac{1}{Z_1} + \frac{1}{Z_2} + \frac{1}{Z_3} + \frac{1}{Z_4}\right), \text{ where, } Z_i = R + j2\pi fL - j\frac{1}{2\pi fC}$$

The wiring used is stranded in nature and is assumed to have the same physical dimensions and similar electrical properties throughout the network. We model the transmitter and receiver that both are depicted in Figure 9 as impedance $\boldsymbol{Z_{in/out}}$, where the impedance value of $Z_{in/out}^{11} = Z_{in/out}^{22} = Z_{in/out}^{12} = Z_{in/out}^{12}$ is equal to $50\ \Omega$.

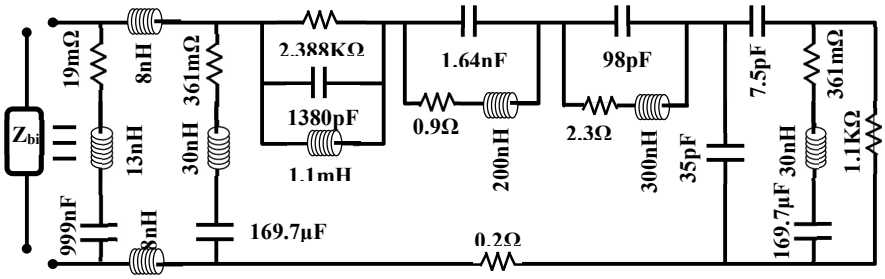

Figure 9 Equivalent impedance for a mobile phone charger.

The basic cable parameters of our experimental network are as follows:

Power line radius (2.5 mm^2): r = 0.89 mm; distance between power lines: d = 2.5 mm

Electric conductivity of conductors: $\sigma = 5.575 \times 10^7$ S/m

Magnetic permeability: $\mu = 4\pi 10^{-7}$ H/m

Permittivity of dielectric: $\varepsilon = \varepsilon_0 \varepsilon_r$ where, $\varepsilon 0 = (1/36\pi).10^{-9}$ F/m is the relative dielectric constant. The vacuum dielectric constant is [24]:

$$\varepsilon_r = \frac{1.6661.10^{-6}}{f} + 2.9701 \quad \text{F/m}$$

The following parameters were considered in our simulation: frequency band: $[1-100]MHz$; number of carrier frequencies: 4125; carrier frequency: $\Delta f = 24KHz$. For NSD, the colored Gaussian noise model described in [5] was considered.

$N_{Rx}(f) = \frac{1}{f^2} + 10^{-15.5}$ mW/Hz ; PSD: $-50dBm/Hz$ from $[1-100]\,MHz$

4.1 Channel Transfer Function

Let us now see the impact of electrical appliances on the channel transfer function. To analyze the behavior of the PLC channel, we used the PLC network represented in Figure 7, where all sockets are in open state, except Socket 4, which is connected with an electrical household appliance that is equivalent to its input impedance Z_{bi}.

The transfer function H^{ij} of the MIMO PLC channel are shown in Figures 10(a), (b), (c) and (d). These transfer function channels are obtained when one socket is in open state or connected to an appliance device.

In this analysis, we considered two types of devices: with and without a plug with PE conductor. The second ones were connected to a socket with N and P wires, i.e., while the N-PE and P-PE connections were open. The results obtained when these devices were connected to the network are shown in Figure 11. From these figures, we can obtain two types of channel responses: from the co-channel and the cross-channel.

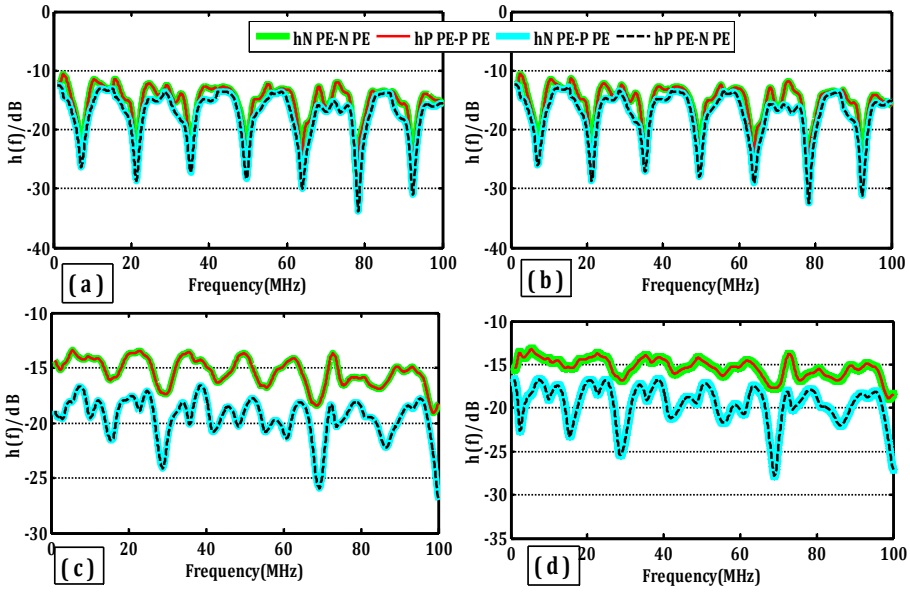

Figure 10 MIMO PLC channel transfer function: (a) lamp, (b) mobile phone charger, (c) electric heater, and (d) micro-computer.

The transfer function of an indoor 2*2 MIMO PLC network was realized from 1 MHz up to 100 MHz. The comparison shows that there was a significant impact of the input impedance connected to the sockets on the behavior of the PLC channel transfer function. Moreover, for the case with the plug with PE conductor we can see that the difference between the co-channel (hN PE-N PE or hP PE-P PE) and the cross-channel (hN PE-P PE or hP PE-N PE) was approximately 5dB, as shown in Figures 11(a) and (b), but this difference was less significant in the cases of devices that had a plug without PE conductor. Thus, the main conclusion from this analysis is that the transfer function of a MIMO PLC channel is influenced by the type of plugs that are connected to the socket. Furthermore, we saw that the transfer function of the MIMO PLC channel displayed strong notches in some frequency bands. Therefore, these bands must be ignored when designing a PLC system, i.e., no useful information should be transmitted over these bands.

4.2 Throughput Over MIMO PLC Channel

After analyzing the behavior of the PLC channel, we will now look at the effect of appliances connected to the PLC network on the data rate supported by the system. As mentioned above, the measured data rate over SISO PLC depends on the type of electrical appliance as well as on the length of the cable. In this subsection, we will calculate the throughput of a MIMO PLC channel and compare it with the throughput of a SISO PLC channel.

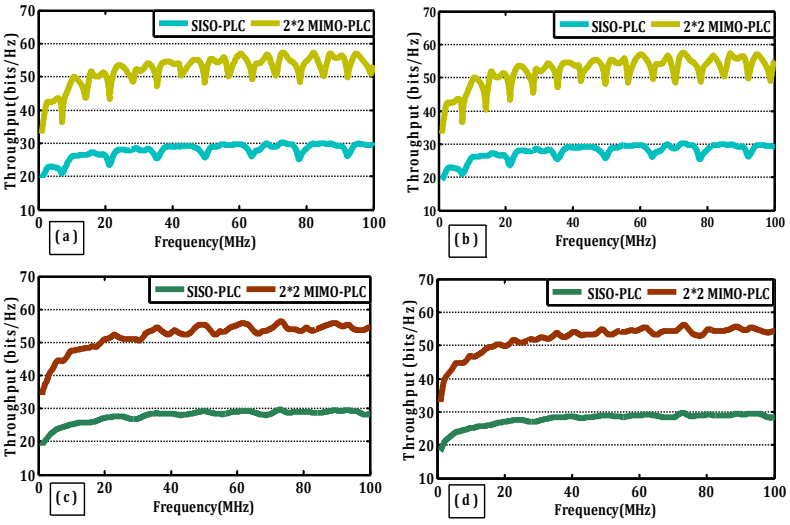

Figure 11 Throughput versus frequency for MIMO PLC and SISO PLC for (a) lamp, (b) mobile phone charger, (c) electric heater, and (d) micro-computer.

Figures 11(a), (b), (c) and (d) give the simulation results for the throughput between the transmitter and the receiver in the MIMO and SISO power line communication networks. These figures show the case for one socket when connected to a lamp, a mobile phone charger, an electric heater, and a micro-computer, respectively. From these figures, it can be seen that the throughput offered by the PLC-MIMO channel was higher than the throughput offered by the SISO PLC channel. In both cases, the throughput increased with frequency. Moreover, by comparing the simulated throughput results shown in Figures 12(a) and (b) (household appliances that have a plug without PE conductor) with the throughput results shown in Figure 11(c) and (d) (household appliances that have a plug with PE conductor), it can be observed that the impact of the devices that have the same plug (two or three conductors) on throughput was only slightly significant. However, when we compare the cases that do not have the same type of plug, for example, the mobile phone charger and micro-computer, we can clearly see the influence of the PE conductor on throughput. Generally, from the figures related to the throughput it seems that the performance of the MIMO PLC system was almost 90% higher than that of the SISO PLC system. In addition, the type of socket plays a major role in determining the throughput of a MIMO PLC system.

5 Conclusion

In this work, we carried out actual measurements of the useful throughput on the proposed SISO PLC network. The measurements that were performed on the different configurations pointed out that the data rate through a PLC network depends not only on the type of modem but also on the nature of the load connected to the network. Besides, we proposed a MIMO system to enhance the throughput of PLC networks. In addition, based on the MTL theory, we obtained a new calculation of the MIMO channel transfer function. This calculation allowed us to see the influences of different household appliances connected across the various sockets of our PLC grid on the throughput in the MIMO PLC network. The throughput in a MIMO PLC network is influenced by several factors, especially the type of terminal load branch, i.e., the kind of plugs of the household appliances connected to the sockets of the MIMO PLC network.

In fact, the effect of the common mode radiation on the behavior of the MIMO PLC channel in terms of throughput is negative, so the longer the line network topologies, the more significant the effect. Therefore, in a future work we will focus on taking this factor into account, where we will add its algorithms to conduct a simulation whose results will approximate reality.

References

[1] Belkadid, J., Benbassou, A. & EL Ghzaoui, M., *PAPR Reduction in CE-OFDM System for Numerical Transmission via PLC Channel*, International Journal on Communications Antenna and Propagation (IRECAP), **3**(5), Oct. 2013, DOI: 10.15866/irecap. v3i5.4255.

[2] Berger, L.T., Schwager, A., Pagani, P. & Schneider, D. M., *MIMO Power Line Communications*, IEEE Communications Surveys Tutorials, **17**(1), pp. 106-124, 2015, DOI: 10.1109/COMST.2014.2339276.

[3] El Ghzaoui, M., Hmamou, A., Foshi, F. & Mestoui, J., *Compensation of Non-linear Distortion Effects in MIMO-OFDM Systems Using Constant Envelope OFDM for 5G Applications*, J. Circuits, Syst. Comput., **29**(16), 2050257, 2020.

[4] Canete, F., Cortes, J., Diez, L. & Entrambasaguas, J., *A Channel Model Proposal for Indoor Power Line Communications*, IEEE Comm Magazine, **49**(12), pp. 166-174, 2011. DOI: 10.1109/MCOM.2011.6094022.

[5] Versolatto, F. & Tonello, A.M., *A MIMO PLC Random Channel Generator and Capacity Analysis*, IEEE International Symposium on Power Line Communications and Its Applications, Udine, Italy, pp. 66-71, Apr. 2011, DOI: 10.1109/ISPLC.2011.5764452.

[6] Corchado, J.A., Cortes, J.A., Canete, F.J. & Diez, L., *An MTL-Based Channel Model for Indoor Broadband MIMO Power Line Communications*, IEEE Journal on Selected Areas in Communications, **34**(7), pp. 2045–2055, Jul. 2016. DOI: 10.1109/JSAC.2016.2566178.

[7] Sadamori, L., Hunziker, T. & Dominiak, S., *Gains and Limits of MIMO Technology for Safety-Critical PLC Applications*, International Symposium on Power Line Communications and its Applications (ISPLC), Bottrop, pp. 81-86, 2016. DOI: 10.1109/ISPLC.2016.7476268.

[8] Mlynek, Misurec, Silhavy, Fujdiak, Slacik, & Hasirci, *Simulation of Achievable Data Rates of Broadband Power Line Communication for Smart Metering*, Applied Sciences, **9**(8), 1527, Apr. 2019. DOI: 10.3390/app9081527.

[9] Duan, X., Wei, Y., He, D., Xu, Z., Zhang, H. & Hua, W., *Research on Channel Model of Broadband Power Line Communication Based on Mtl and Radiation Effect*, Progress in Electromagnetics Research M, **92**, pp. 67-78, 2020, DOI: 10.2528/PIERM20011002.

[10] Qian, Y., Zhou, X., Li, J., Shu, F. & Jayakody, D.N.K., *A Novel Precoding and Impulsive Noise Mitigation Scheme for MIMO Power Line Communication Systems*, IEEE Systems Journal, **13**(1), pp. 6-17, Mar. 2019.DOI: 10.1109/JSYST.2018.2880962.

[11] Kasthala, S. & Venkatesan, P. G.K.D, *Evaluation of Channel Modeling Techniques for Indoor Power Line Communication*, Progress in Advanced

Computing and Intelligent Engineering, **564**, Springer Singapore, pp. 577-587, 2018. DOI: 10.1007/978-981-10-6875-1_57.

[12] Benaissa, A., Abdelmalek, A., Feham, M., Himeur, Y. & Boukabou, B., *Hybrid Forward Error Correction Coding Efficiency for MIMO PLC with Symmetric Alpha-Stable Noise*, Telecommunication Systems, **75**(3), pp. 319-329, Nov. 2020, DOI: 10.1007/s11235-020-00685-7.

[13] Fadaei Tehrani, A., Yeh, H.G. & Kwon, S.C., *BER Performance of Space–Time Parallel ICI Cancellation of OFDM in MIMO Power Line Communications*, IEEE Systems Journal, **15**(2), pp. 1742-1752, Jun. 2021. DOI: 10.1109/JSYST.2020.2968542.

[14] Masood, B., Guobing, S., Naqvi, R.A., Rasheed, M.B., Hou, J. & Rehman, A.U., *Measurements and Channel Modeling of Low and Medium Voltage NB-PLC Networks for Smart Metering*, IET Generation, Transmission & Distribution, **15**(2), pp. 321-338, Jan. 2021. DOI: 10.1049/gtd2.12023.

[15] García-Gangoso, F., Blanco-Velasco, M., & Cruz-Roldán, F., *Formulation and Performance Analysis of Broadband and Narrowband OFDM-Based PLC Systems*, Sensors, **21**(1), 290, Jan. 2021. DOI: 10.3390/s21010290.

[16] Mestoui, J., El ghzaoui, M., Hmamou, A., & Foshi, J. *BER Performance Improvement in CE-OFDM-CPM System using Equalization Techniques over Frequency-Selective Channel*, Procedia Computer Science, 151, 1016-1021, 2019.

[17] Chariag, D., Bunetel, J.C.L. & Raingeaud, Y., *A Method to Construct Equivalent Circuit from Input Impedance of Household-Appliances*, International Journal on Communications Antenna and Propagation, **2**(4), pp. 226-235, 2012.

[18] Papaleonidopoulos, I.C., Karagiannopoulos, C.G. & Theodorou, N.J., *A Theoretical Justification of the Two-Conductor HF Transmission-Line Model for Indoor Single-Phase Low Voltage Triplex Cables*, International Symposium on Power-line Communications and its Applications, pp. 114-119, Japan, 2007.

[19] Franek, L., Stastny, L., Kaczmarczyk, V. & Bradac, Z., *Multiwire Power Line Communication Model*, IFAC-PapersOnLine, **48**(4), pp. 147-152, 2015. DOI: 10.1016/j.ifacol.2015.07.023.

[20] Franek, L. & Fiedler, P., *A Multiconductor Model of Power Line Communication in Medium-Voltage Lines*, Energies, **10**(6), 816, Jun. 2017. DOI: 10.3390/en10060816.

[21] Hassan, E.S., *Multi User MIMO-OFDM Based Power Line Communication Structure with Hardware Impairments and Crosstalk*, IET Communications, **11**(9), pp. 1466-1476, Jun. 2017. DOI: 10.1049/iet-com.2016.0952.

[22] Mestoui, J., El Ghzaoui, M., Fattah, M., Hmamou, A. & Foshi, F., *Performance Analysis Of CE-OFDM-CPM Modulation using MIMO*

System over Wireless Channels, J Ambient Intell Human Comput., **11**, pp. 3937-3945, 2020. DOI: 10.1007/s12652-019-01628-0.

[23] Tarateeraseth, V., Maio, I.A. & Canavero, F.G., *Assessment of Equivalent Noise Source Approach for EMI Simulations of Boost Converter*, 20th International Zurich Symposium on Electromagnetic Compatibility, Zurich, Switzerland. pp. 353-356, Jan. 2009. DOI: 10.1109/EMCZUR. 2009.4783463.

[24] Versolatto, F. & Tonello, A.M., *An MTL Theory Approach for the Simulation of MIMO Power-Line Communication Channels*, IEEE Transactions on Power Delivery, **26**(3), pp. 1710-1717, Jul. 2011.